Observation of linear, nonlinear and singular behavior of the Pancharatnam-Berry phase

T. van Dijk[a], H.F. Schouten[a], W. Ubachs[a] and T.D. Visser[a,b]

[a]Dept. of Physics and Astronomy, and Laser Centre, Free University,
De Boelelaan 1081, 1081 HV Amsterdam, The Netherlands
[b]Dept. of Electrical Engineering, Delft University of Technology,
Mekelweg 4, 2628 CD Delft, The Netherlands

ABSTRACT

If the state of polarization of a monochromatic light beam is changed in a cyclical manner, the beam acquires–in addition to the usual dynamic phase–a *geometric phase*. This so-called *Pancharatnam-Berry phase*, equals half the solid angle of the contour traced out on the Poincaré sphere. We show that such a geometric interpretation also exists for the *Pancharatnam connection*, the criterion according to which two beams with different polarization states are said to be in phase. This interpretation offers a new and intuitive method to calculate the geometric phase that accompanies non-cyclic polarization changes. We also present a novel setup that allows the observation of the geometric phase for such changes. The phase can depend in a linear or in a nonlinear fashion on the orientation of the optical elements, and sometimes the dependence is singular. Experimental results that confirm these three types of behavior are presented. The observed singular behavior may be applied in the design of optical switches.

Keywords: Polarization, Geometric phase, Optical switching

1. INTRODUCTION

In 1984 Berry pointed out that a quantum system whose parameters are cyclically altered does not return to its original state but acquires, in addition to the usual dynamic phase, a so-called geometric phase.[1] It was soon realized that such a phase is not just restricted to quantum systems, but also occurs in contexts such as Foucault's pendulum.[2] Also the polarization phenomena described by Pancharatnam[3] represent one of its manifestations. The polarization properties of a monochromatic light beam can be represented by a point on the Poincaré sphere.[4] When, with the help of optical elements such as polarizers and retarders, the state of polarization is made to trace out a closed contour on the sphere, the beam acquires a geometric phase. This *Pancharatnam-Berry phase*, as it is nowadays called, is equal to half the solid angle of the contour subtended at the origin of the sphere.[5–8]

In this work we show that such a geometric relation also exists for the so-called *Pancharatnam connection*, the criterion according to which two beams with different polarization states are in phase, i.e., their superposition produces a maximal intensity. This relation can be extended to arbitrary (e.g., non-closed) paths on the Poincaré sphere, and allows us to study how the phase builds up for such non-cyclic polarization changes. Our work offers an geometry-based alternative to the algebraic work presented earlier.[9,10] We also discuss how the geometric phase for non-cyclic polarization changes can depend in a linear, a nonlinear or in a singular fashion on the orientation of the optical elements. Experimental results obtained with a new interferometric setup that confirm these three types of behavior are presented. The observed singular behavior may be applied in the design of fast optical switches.

T.D. Visser's email address is t.d.visser@tudelft.nl

Complex Light and Optical Forces IV, edited by Enrique J. Galvez, David L. Andrews, Jesper Glückstad,
Proc. of SPIE Vol. 7613, 76130E · © 2010 SPIE · CCC code: 0277-786X/10/$18 · doi: 10.1117/12.840871

2. GEOMETRY OF THE PANCHARATNAM CONNECTION

The state of polarization of a monochromatic beam can be represented as a two-dimensional Jones vector[11] with respect to an orthonormal basis $\{\hat{\mathbf{e}}_1, \hat{\mathbf{e}}_2\}$, as

$$\mathbf{E} = \cos\alpha\,\hat{\mathbf{e}}_1 + \sin\alpha\exp(\mathrm{i}\theta)\,\hat{\mathbf{e}}_2, \tag{1}$$

with $0 \leq \alpha \leq \pi/2$; $-\pi \leq \theta \leq \pi$, and $\hat{\mathbf{e}}_i \cdot \hat{\mathbf{e}}_j = \delta_{ij}, (i,j = 1,2)$. The angle α is a measure of the relative amplitudes of the two components of the electric vector $\mathbf{E}$, and the angle θ denotes their phase difference. Two different states of polarization, A and B, can hence be written as

$$\mathbf{E}_A = \left(\cos\alpha_A, \sin\alpha_A e^{\mathrm{i}\theta_A}\right)^T, \tag{2}$$

$$\mathbf{E}_B = e^{\mathrm{i}\gamma_{AB}}\left(\cos\alpha_B, \sin\alpha_B e^{\mathrm{i}\theta_B}\right)^T. \tag{3}$$

Since only relative phase differences are of concern, the overall phase of $\mathbf{E}_A$ in Eq. (2) is taken to be zero. According to Pancharatnam's connection[5] these two states are in phase when their superposition yields a maximal intensity, i.e., when

$$|\mathbf{E}_A + \mathbf{E}_B|^2 = |\mathbf{E}_A|^2 + |\mathbf{E}_B|^2 + 2\,\mathrm{Re}(\mathbf{E}_A \cdot \mathbf{E}_B^*) \tag{4}$$

reaches its greatest value, implying that

$$\mathrm{Im}\,(\mathbf{E}_A \cdot \mathbf{E}_B^*) = 0, \tag{5}$$

$$\mathrm{Re}\,(\mathbf{E}_A \cdot \mathbf{E}_B^*) > 0. \tag{6}$$

These two conditions uniquely determine the phase γ_{AB}, except when the states A and B are orthogonal.

Let us now consider a sequence of three polarization states with each succesive state being in phase with its predecessor. As the initial state we take the basis-state X with Jones vector $\mathbf{E}_X = (1,0)^T$. It follows immediately that *any polarization state A with Jones vector $\mathbf{E}_A$ as defined by Eq. (2) is in phase with X.* Consider now a third state B. This state is in phase with A provided that the angle γ_{AB} in Eq. (3) satifies the relations (5) and (6). Clearly, B is not in phase with X, but rather with $e^{\mathrm{i}\gamma_{AB}}X$. Apparently the total geometric phase that is accrued by following the closed circuit XAB equals γ_{AB}. This observation allows us to make use of Pancharatnam's classic result which relates the accumulated geometric phase to the solid angle of the geodesic triangle XAB.[3] According to this result then, the angle (phase) γ_{AB} between the states A and B for which they are in phase is given by half the solid angle Ω_{XAB} of the triangle XAB subtended at the center of the Poincaré sphere, i.e.,

$$\gamma_{AB} = \Omega_{XAB}/2. \tag{7}$$

The solid angle Ω_{XAB} is taken to be positive (negative) when the the circuit XAB is traversed in a counter-clockwise (clockwise) manner. Thus we have $-2\pi \leq \Omega_{XAB} \leq 2\pi$, and hence $-\pi \leq \gamma_{AB} \leq \pi$. Hence we arrive at the following geometric interpretation of Pancharatnam's connection: *The phase γ_{AB} for which the superposition of two beams with polarization states A and B yields a maximum intensity, equals half the solid angle subtended by their respective Stokes vectors and the Stokes vector corresponding to the basis-state X.* We emphasize that γ_{AB} is defined with respect to a certain basis. We return to this point later.

Several consequences follow from the geometric interpretation. First, consider a state B that lies on the great circle through the points A and X. Two cases can be distinguished. If B is not on the geodesic that connects $-A$ and $-X$, then the curves XA, AB and BX cancel each other, i.e., $\gamma_{AB} = \Omega_{XAB}/2 = 0$. If B does lie on the geodesic connecting $-A$ and $-X$, then these three curves together constitute the entire great circle and hence $\gamma_{AB} = \Omega_{XAB}/2 = \pi$. Consequently, we arrive at

Corollary 1. *All polarization states that lie on the great circle that runs through A and X and which are not part of the geodesic curve that connects $-A$ and $-X$ are in phase with state A. All other states on the great circle are out of phase with state A.*

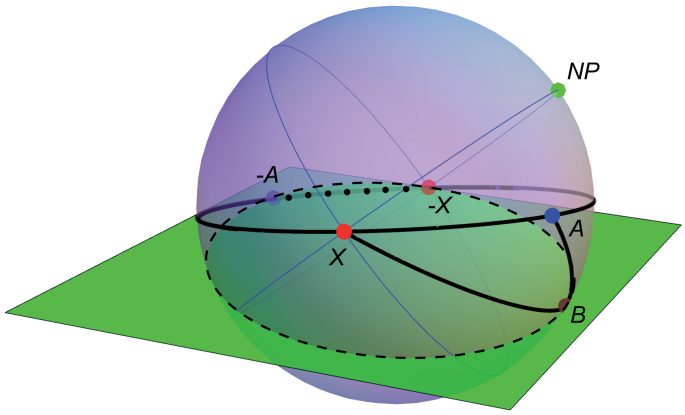

Figure 1. Illustrating the intersection of the plane given by Eq. (10) and the Poincaré sphere. This intersection is a circle (indicated by the dashed curve) that runs through the points $-A$, $-X$ and B. All points on the circle segment that runs from $-A$ to B to $-X$ constitute the set $\{B'\}$ of states that have the same phase difference γ_{AB} with respect to A as the state B. The great circle through A and X is shown solid-dotted. The point NP indicates the North Pole.

(We exlude the pathological case $A = \pm X$.)

COROLLARY 2. *The great circle that runs through A and X divides the Poincaré sphere into two halves, one on which all states have a positive phase with respect to A, and one on which all states have a negative phase with respect to A.*

Thus far we not specified the basis vectors in which the Jones vectors are expressed. The two most commonly used are the cartesian representation and the helicity representation. The Stokes vector corresponding to the basis-state X is $(1, 0, 0)$ and $(0, 0, 1)$ in these two bases, respectively. Our results so far are valid for any choice of representation. For computational ease, however, we will from now on make use of the cartesian basis.

Given two different polarization states A and B, we may enquire about the set $\{B'\}$ of all states which have the same phase difference γ_{AB} with respect to A as B has. We begin by noticing that the solid angle Ω_{ABC} subtended at the origin of the Poincaré sphere by three unit vectors $\mathbf{A}$, $\mathbf{B}$ and $\mathbf{C}$ satisfies the equation[12]

$$\tan\left(\frac{\Omega_{ABC}}{2}\right) = \frac{\mathbf{A}\cdot(\mathbf{B}\times\mathbf{C})}{1+\mathbf{B}\cdot\mathbf{C}+\mathbf{A}\cdot\mathbf{C}+\mathbf{A}\cdot\mathbf{B}}. \tag{8}$$

On taking $\mathbf{A}$, $\mathbf{B}$ and $\mathbf{C}$ as the Stokes vectors corresponding to states A, B, and X, i.e., $\mathbf{C} = (1, 0, 0)$, Eqs. (7) and (8) yield

$$\tan\gamma_{AB} = \frac{A_y B_z - A_z B_y}{1 + B_x + A_x + A_x B_x + A_y B_y + A_z B_z}. \tag{9}$$

For γ_{AB} and $\mathbf{A}$ fixed, we thus find that the three components of $\mathbf{B}$ must satisfy the relation

$$c_x B_x + c_y B_y + c_z B_z + D = 0, \tag{10}$$

with the coefficients c_x, c_y, c_z and D given by

$$\begin{aligned} c_x &= \tan\gamma_{AB}(1 + A_x), && (11)\\ c_y &= \tan\gamma_{AB} A_y + A_z, && (12)\\ c_z &= \tan\gamma_{AB} A_z - A_y, && (13)\\ D &= c_x. && (14) \end{aligned}$$

The solutions of Eq. (10) form a plane. In addition, the vector $\mathbf{B}$ must be of unit length, ensuring that it lies on the Poincaré sphere. The intersection of the plane and the sphere is a circle that runs through B. Finding

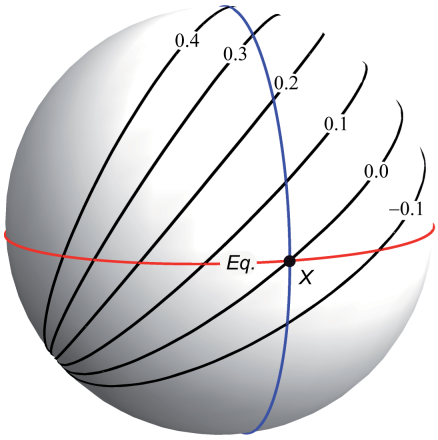

Figure 2. Selected contours of the phase γ_{AB} for the case $\mathbf{A} = (0, 0.8, 0.6)$. The basis-state X, the equator ($Eq.$) and the meridian through X are also shown.

two other point on this circle defines it uniquely. It can be verified by substitution that the Stokes vectors $-\mathbf{A}$ and $-\mathbf{X}$ both satisfy Eq. (10). Hence, for all states on the circle that runs through B, $-A$ and $-X$, the phase γ_{AB} has the same value, mod π. Since the plane defined by Eq. (10) does, in general, not include the origin of the Poincaré sphere, this circle is not a great circle. This is illustrated in Fig. 1, where the circle through B is drawn dashed. This circle intersects the great circle through A and X at the points $-A$ and $-X$. According to Corollary 2, γ_{AB} changes sign at these points. Since Eq. (9) defines the phase modulo π, it follows that γ_{AB} undergoes a π phase jump at these points. We thus arrive at

Corollary 3. *Consider the circle through $-A$, $-X$ and B. It consists of two segments, both with endpoints $-A$ and $-X$. The segment which includes B equals the set $\{B'\}$ of states such that $\gamma_{AB'} = \gamma_{AB}$. The other segment represents states for which $\gamma_{AB'} = \gamma_{AB} \pm \pi$.*

It can be shown that the plane-sphere intersection is always a circle, and not just a single point, if the pathological case $A = \pm X$ is excluded. If, for a fixed state A, the state B is being varied, the plane given by Eq. (10) rotates along the line connecting $-A$ and $-X$.

We now demonstrate how our geometric interpretation implies that for a fixed state A the phase γ_{AB} may vary in different ways when the state B is moved across the Poincaré sphere. We specify the position of B by spherical coordinates (ϕ, θ), where $0 \leq \phi \leq 2\pi$ and $0 \leq \theta \leq \pi$ represent the azimuthal angle and the angle of inclination, respectively. If A is taken to be at the south pole and $B = B(\phi)$ lies on the equator, then

$$\gamma_{AB} = \frac{\Omega_{XAB}}{2} = \frac{1}{2}\int_{\pi/2}^{\pi}\int_{0}^{\phi} \sin\theta \, \mathrm{d}\phi' \mathrm{d}\theta = \frac{1}{2}\phi. \tag{15}$$

Clearly, the phase varies linearly with the angle ϕ in this case.

Let us now consider the contours of equal phase γ_{AB} as shown in Fig. 2. It is seen that the intersections of the contours with the equator are not equidistant. Hence in this case the phase depends in a non-linear way on the angle ϕ.

The singular behavior, finally, of the phase is a direct consequence of the fact that two anti-podal states A and $-A$ do not interfere with each other [see the remark below Eq. (6)]. From Eq. (8) it follows that the phase is antisymmetric under the interchange of the points $\mathbf{C} = \mathbf{X}$ and $\mathbf{A}$. Hence we expect two singular points, namely $-A$ and $-X$, with opposite topological charge (± 1). This is illustrated in Figs. 3 and 4. We note that the existence of singular points is in agreement with the "Hairy Ball Theorem" due to Brouwer,[13] according to which there is no nonvanishing continuous tangent vector field on a sphere in $\mathbb{R}^3$. This implies that $\nabla\gamma_{AB}$ has at least one zero, in this case at the two singularities.

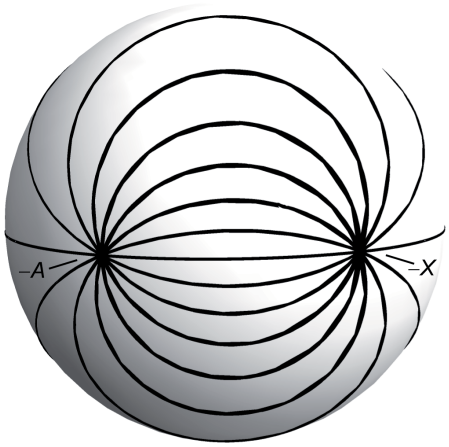

Figure 3. Contours of equal phase of γ_{AB} for the case that the state A is taken to be $(0.6, 0, 0.8)$. Two singular points with opposite topological charge can be seen at $-A$ and $-X$.

3. NON-CYCLIC POLARIZATION CHANGES

Let us now apply our results for the Pancharatnam connection to study the geometric phase for an arbitrary, i.e. non-closed, path ABC on the Poincaré sphere. The successive states are assumed to be in phase. Therefore the geometric phase accumulated on this path equals

$$\begin{aligned} \gamma_{ABC} \equiv \gamma_{AB} + \gamma_{BC} &= (\Omega_{XAB} + \Omega_{XBC})/2, \\ &= \Omega_{XABC}/2, \end{aligned} \tag{16}$$

where Ω_{XABC} is the *generalized solid angle* of the path $X \to A \to B \to C \to X$. Ω_{XABC} can consist of two triangles (see Fig. 5), whose contribution is positive or negative depending on their handedness.

Now we keep states A and C fixed, and study how the geometric phase γ_{ABC} changes when state B is varied. We will show that this change, in contrast to γ_{AB}, is independent of the choice of basis vectors. Consider the phase γ'_{ABC} in a non-cartesian basis (for example, the helicity basis) whose first basis state we call N. We then

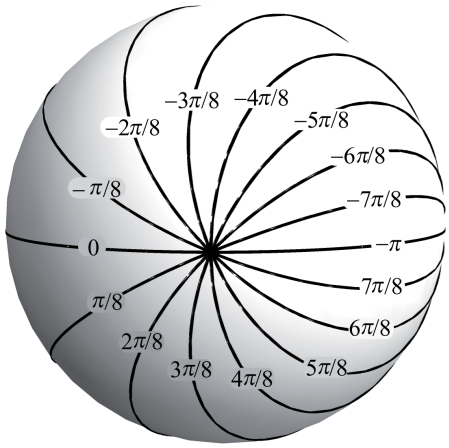

Figure 4. Contours of equal phase of γ_{AB} for the case that the state A is taken to be $(0, 0, 1)$. The singularity at $-A$ is seen to have topological charge $+1$.

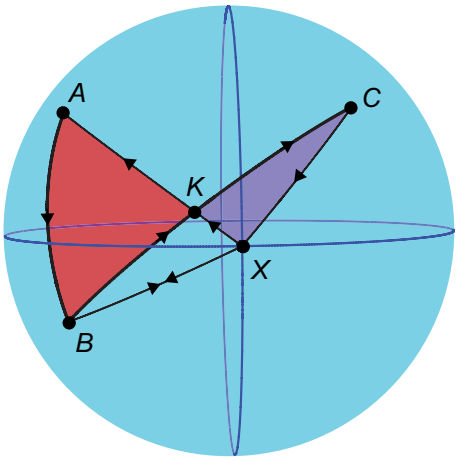

Figure 5. Illustrating the generalized solid angle Ω_{XABC}. In going from state A to state B, the beam acquires a geometric phase equal to half the solid angle Ω_{XAB}, which is positive. In going from B to C the acquired phase equals half the solid angle Ω_{XBC}, which is negative. Since the triangle BKX does not contribute, this is equivalent to the generalized solid angle Ω_{XABC}, which equals half the solid angle of the triangle ABK (positive), plus half the solid angle of the triangle XKC (negative).

have, in analogy to Eq. (16),

$$\begin{aligned} \gamma'_{ABC} \equiv \gamma'_{AB} + \gamma'_{BC} &= (\Omega_{NAB} + \Omega_{NBC})/2, \\ &= \Omega_{NABC}/2. \end{aligned} \tag{17}$$

Also,

$$\Omega_{NABC} - \Omega_{XABC} = \Omega_{NABC} + \Omega_{CBAX} = \Omega_{NAXC}. \tag{18}$$

The justification of the last step of Eq. (18) is illustrated in Fig. 6. It follows on using Eqs. (16)–(18) that

$$\gamma'_{ABC} - \gamma_{ABC} = \Omega_{NAXC}/2. \tag{19}$$

The term $\Omega_{NAXC}/2$ is a constant, independent of B, i.e. the geometric phase in both reprensentations differs by a constant only. Hence the variation of the geometric phase with B is independent of the choice of basis, as it

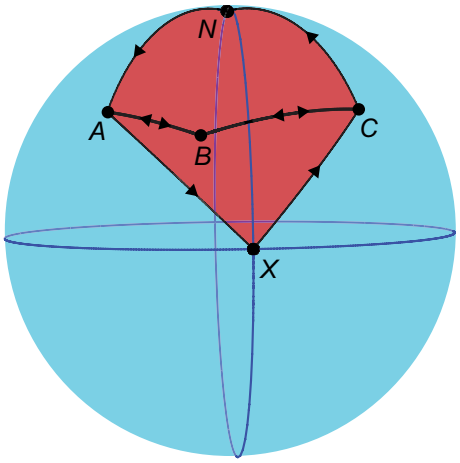

Figure 6. Illustrating the equality $\Omega_{NABC} + \Omega_{CBAX} = \Omega_{NAXC}$. Such a construction can be made for any choice of states.

should be for an observable quantity. This is in contrast to γ_{AB}, which explicitly depends on the choice of basis, as is evident from Eqs. (2–3).

The behavior of γ_{ABC} on varying B can be linear,[14] non-linear[15] or singular,[16–18] as we have also shown for γ_{AB}. However γ_{AB} has singularities at $B = -A$ and $B = -X$. The first is due to the orthogonality of A and $-A$, while the second is a consequence of the choice of representation. The phase γ_{ABC} is singular only at $B = -A$ and $B = -C$, and not at $B = -X$.

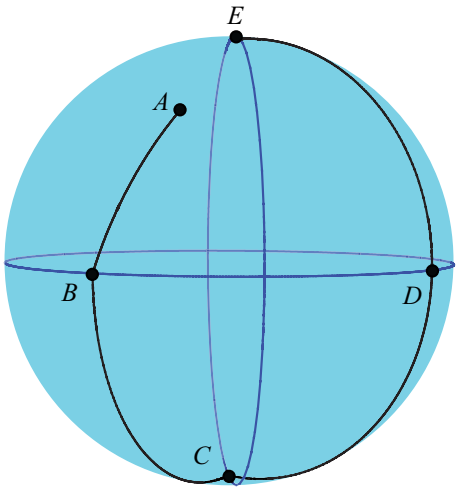

Figure 7. Non-closed path $ABCDE$ on the Poincaré sphere for a monochromatic light beam that passes through a sequence of polarizers and compensators.

4. ALGEBRA OF THE PANCHARATNAM-BERRY PHASE

We again study a series of polarization changes for which the successive states are assumed to be in phase, but now we employ algebraic methods.

To illustrate the rich behavior of the geometric phase, consider a beam in an arbitrary initial state A, that passes through a linear polarizer whose transmission axis is under an angle ϕ_1 with the positive x-axis. This results in a second state B that lies on the equator of the Poincaré sphere (see Fig. 7). Next the beam passes through a suitably oriented compensator, which produces a third, left-handed circularly polarized state C on the south pole. The action of a second linear polarizer, with orientation angle ϕ_2, creates state D on the equator. Finally, a second compensator causes the polarization to become right-handed circular, corresponding to the state E on the north pole. These successive manipulations can be described with the help of Jones calculus.[11,19] The matrix for a linear polarizer whose transmission axis is under an angle ϕ with the positive x-axis equals

$$\mathbf{P}(\phi) = \begin{pmatrix} \cos^2\phi & \cos\phi\sin\phi \\ \cos\phi\sin\phi & \sin^2\phi \end{pmatrix}, \tag{20}$$

whereas the matrix for a compensator ("retarder") with a fast axis under an angle θ with the positive x-axis, which introduces a phase change δ between the two field components is

$$\mathbf{C}(\delta,\theta) = \begin{pmatrix} \cos(\delta/2) + \mathrm{i}\sin(\delta/2)\cos(2\theta) & \mathrm{i}\sin(\delta/2)\sin(2\theta) \\ \mathrm{i}\sin(\delta/2)\sin(2\theta) & \cos(\delta/2) - \mathrm{i}\sin(\delta/2)\cos(2\theta) \end{pmatrix}. \tag{21}$$

The (unnormalized) Jones vector for the final state E thus equals

$$\mathbf{E}_E = \mathbf{C}(\pi/2, \phi_2 - \pi/4) \cdot \mathbf{P}(\phi_2) \cdot \mathbf{C}(-\pi/2, \phi_1 - \pi/4) \cdot \mathbf{P}(\phi_1) \cdot \mathbf{E}_A. \tag{22}$$

Hence we find for the normalized states the expressions

$$\mathbf{E}_B = \mathbf{P}(\phi_1)\cdot\mathbf{E}_A = T(A,\phi_1)\begin{pmatrix}\cos\phi_1\\ \sin\phi_1\end{pmatrix}, \tag{23}$$

$$\mathbf{E}_C = \mathbf{C}(-\pi/2,\phi_1-\pi/4)\cdot\mathbf{E}_B = T(A,\phi_1)e^{-\mathrm{i}\phi_1}\begin{pmatrix}1/\sqrt{2}\\ \mathrm{i}/\sqrt{2}\end{pmatrix}, \tag{24}$$

$$\mathbf{E}_D = \mathbf{P}(\phi_2)\cdot\mathbf{E}_C = T(A,\phi_1)e^{\mathrm{i}(\phi_2-\phi_1)}\begin{pmatrix}\cos\phi_2\\ \sin\phi_2\end{pmatrix}, \tag{25}$$

$$\mathbf{E}_E = \mathbf{C}(\pi/2,\phi_2-\pi/4)\cdot\mathbf{E}_D = T(A,\phi_1)e^{\mathrm{i}(2\phi_2-\phi_1)}\begin{pmatrix}1/\sqrt{2}\\ -\mathrm{i}/\sqrt{2}\end{pmatrix}, \tag{26}$$

where

$$T(A,\phi_1) = \frac{\cos\alpha_A\cos\phi_1+\sin\alpha_A e^{\mathrm{i}\theta_A}\sin\phi_1}{|\cos\alpha_A\cos\phi_1+\sin\alpha_A e^{\mathrm{i}\theta_A}\sin\phi_1|} \tag{27}$$

is the (normalized) projection of the initial state A onto the state $(\cos\phi_1,\sin\phi_1)^T$. Although in general the output produced by a compensator is not in phase with the input, it is easily verified with the help of Eqs. (5) and (6) that in this example all consecutive states are indeed in phase. Hence it follows from Eq. (26), that we can identify the quantity

$$\Psi = \arg[T(A,\phi_1)e^{\mathrm{i}(2\phi_2-\phi_1)}] \tag{28}$$

as the geometric phase of the final state E. When a beam in this state is combined with a beam in state A, the intensity equals [cf. Eq. (4)]

$$|\mathbf{E}_A|^2+|\mathbf{E}_E|^2+2\,\mathrm{Re}(\mathbf{E}_A\cdot\mathbf{E}_E^*) = 1+|T(A,\phi_1)|^2+2H(A,\phi_1)\cos(2\phi_2-\phi_1+\phi_H), \tag{29}$$

where

$$H(A,\phi_1)e^{\mathrm{i}\phi_H} = T^*(A,\phi_1)\mathbf{E}_A\cdot\begin{pmatrix}1/\sqrt{2}\\ \mathrm{i}/\sqrt{2}\end{pmatrix}, \tag{30}$$

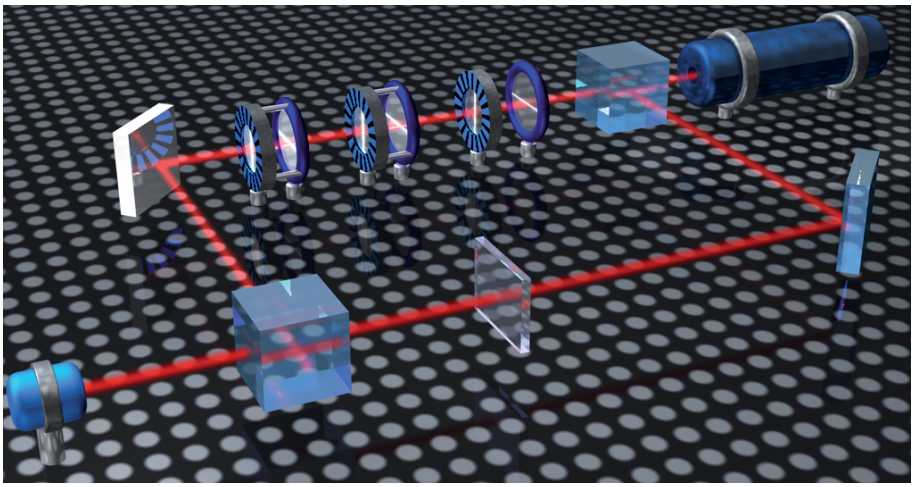

Figure 8. Sketch of the Mach-Zehnder setup. The light from a He-Ne laser (right-hand top) is split into two beams. All polarizing elements are placed in the upper arm, the lower arm only contains a gray filter. The compensators are depicted with striped holders, the linear polarizers with non-striped holders. The last two pairs of elements are mounted together. The interference pattern of the recombined beams is recorded with either a photo diode or a CCD camera (left-hand bottom).

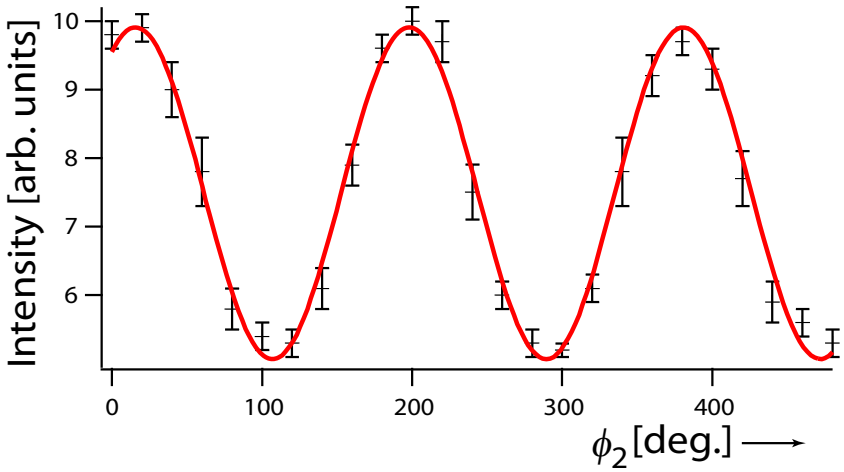

Figure 9. Measured intensity as a function of the orientation angle ϕ_2. The solid curve is a fit of the measured data to the function $C_1 + C_2 \cos(2\phi_2 + C_3)$. The vertical symbols indicate error bars.

and with $H(A, \phi_1) \in \mathbb{R}^+$. In the next section we investigate the dependence of the geometric phase of the final state E on the initial state A, and its dependence on the two orientation angles ϕ_1 and ϕ_2. We also test our predictions experimentally.

5. EXPERIMENTAL METHOD

The above sequence of polarization changes can be realized with a Mach-Zehnder interferometer (see Fig. 8). The output of a He-Ne laser operating at 632.8 nm is divided into two beams. The beam in one arm passes through a linear polarizer and a quarter-wave plate. This produces state A. By rotating the plate, this initial polarization state can be varied. Next the field passes through a polarizer $P(\phi_1)$ that creates state B, and a compensator C_1, resulting in state C. A polarizer $P(\phi_2)$ produces state D, and a compensator C_2 creates the final state E. The elements $P(\phi_1), C_1$ and $P(\phi_2), C_2$ are joined pairwise to ensure that their relative orientation remains fixed when the angles ϕ_1 and ϕ_2 are varied, and the resulting states are circularly polarized. The field in the other arm is attenuated by a gray filter in order to increase the sharpness of the fringes. The fields in both arms are combined, and the ensuing interference pattern is detected with the help of a detector. Both a photodiode and a CCD camera are used.

On varying the angle ϕ_2, the intensity in the upper arm of Fig. 8 remains unchanged and the changes in the diffraction pattern can be recorded with a photodiode. However, when the angle ϕ_1 is varied, the intensity in that arm changes. The shape of the interference pattern then changes as well, and the geometric phase can only be observed by measuring a shift of the *entire* pattern with a CCD camera.[20]

One has to make sure that rotating the optical elements does not affect the optical path length and introduces an additional dynamic phase. This was achieved by an alignment procedure in which the invariance of the interference pattern for 180° rotations of the linear polarizers was exploited. Mechanical vibrations were minimized by remotely controlling the optical elements.

6. EXPERIMENTAL RESULTS

The dependence of the geometric phase of the final state E on the orientation angles ϕ_1 and ϕ_2 of the two polarizers is markedly different. It is seen from Eq. (28) that the phase is proportional to ϕ_2. This linear behavior is illustrated in Fig. 9 in which the intensity observed with a photodiode is plotted as a function of the angle ϕ_2. The solid curve is a fit of the data to the function $C_1 + C_2 \cos(2\phi_2 + C_3)$, with C_1, C_2 and C_3 all constants [cf. Eq. (29)]. The excellent agreement between the measurements and the fitted curve show that the geometric phase Ψ indeed increases twice as fast as the angle ϕ_2.

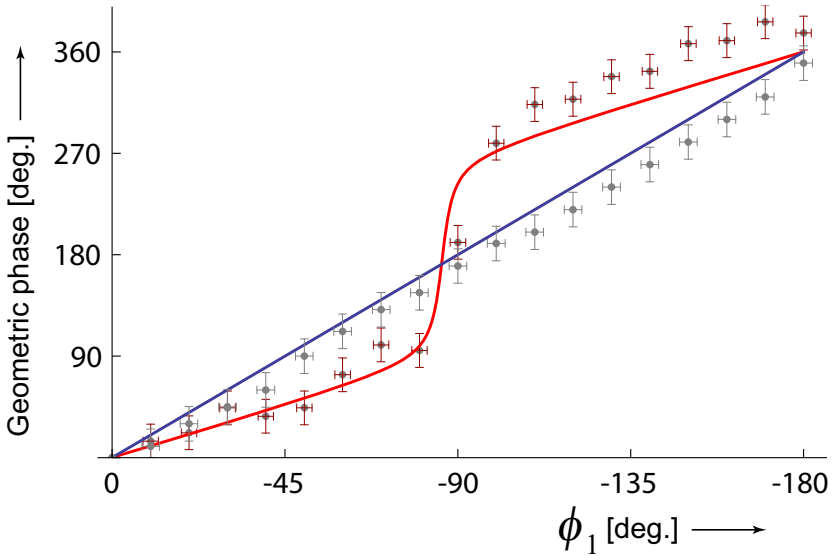

Figure 10. Geometric phase of the final state E when the initial state A coincides with the north pole (blue curve), and when A lies between the equator and the north pole (red curve), both as a function of the orientation angle ϕ_1. The solid curves are theoretical predictions [Eq. (28)], the dots and error bars represent measurements. In this example $\phi_2 = 0$.

In order to investigate the change $\Delta\Psi$ when the angle ϕ_1 is varied from 0° to 180° (after which the polarizer returns to its original state), let us first assume that the initial state A coincides with the north pole (i.e., $\alpha_A = \pi/4, \theta_A = -\pi/2$). In that case the path on the Poincaré sphere is closed and we find from Eq. (28) that $\Psi = 2(\phi_2 - \phi_1)$. The solid angle of the traversed path is now $4(\phi_2 - \phi_1)$. Thus we see that in that case we retrieve Pancharatnam's result that the acquired geometric phase for a closed circuit equals half the solid angle of the circuit subtended at the sphere's origin. Hence, on rotating ϕ_1 over 180°, the accrued geometric phase $\Delta\Psi$ equals 360°. This predicted behavior is indeed observed, see Fig. 10 (blue curve). For an arbitrary initial state on the northern hemisphere [in this example, with Stokes vector $(0.99, -0.14, 0.07)$] the behavior is nonlinear, but again we find that $\Delta\Psi = 360°$ after the first polarizer has been rotated over 180°, see Fig. 10 (red curve).

Let us next assume that the initial state A coincides with the south pole ($\alpha_A = \pi/4, \theta_A = \pi/2$). In that

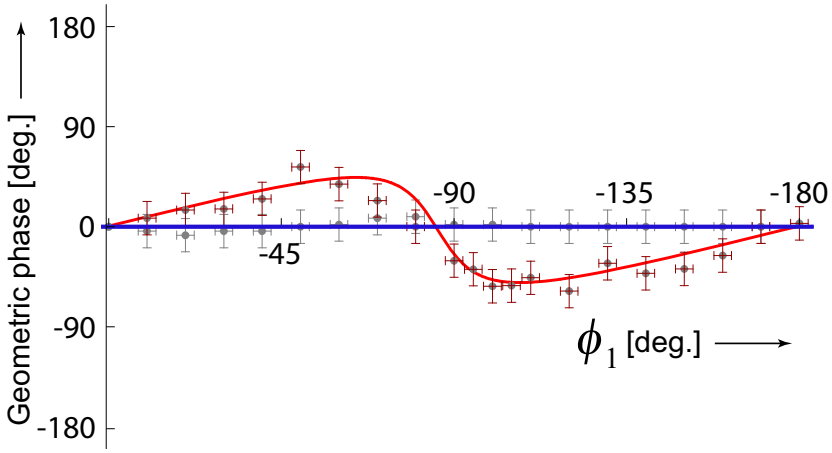

Figure 11. Geometric phase of the final state E when the initial state A coincides with the south pole (blue curve), and when A lies between the equator and the south pole (red curve), both as a function of the orientation angle ϕ_1. The solid curves are theoretical predictions [Eq. (28)], the dots and error bars represent measurements. In this example $\phi_2 = 0$.

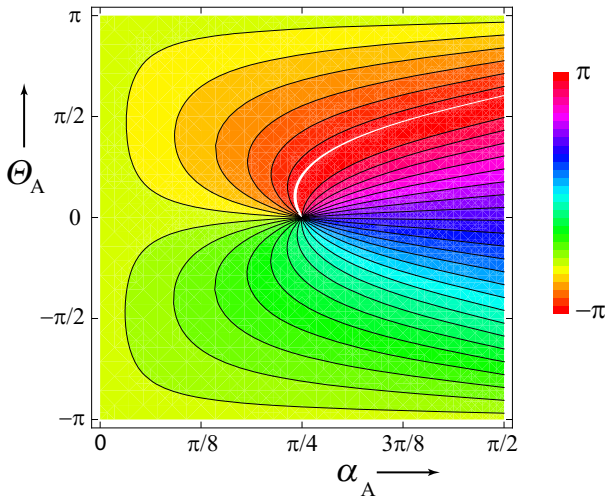

Figure 12. Color-coded plot of the phase of the final state E as a function of the initial state A as described by the two parameters α_A and θ_A [cf. Eq. (2)]. In this example $\phi_1 = 3\pi/4$, and $\phi_2 = 1.8$.

case, Eq. (28) yields $\Psi = 2\phi_2$. Since this is independent of ϕ_1, a rotation of ϕ_1 over 180° results in $\Delta\Psi = 0°$. This corresponds to the blue curve in Fig. 11. For an arbitrary initial state on the southern hemisphere [in this example, with Stokes vector $(0.93, 0.23, -0.28)$] the geometric phase does vary with ϕ_1, but again $\Delta\Psi = 0°$ after a 180° rotation of the polarizer $P(\phi_1)$, see Fig. 11 (red curve). So, depending on the initial polarization state A, topologically different types of behavior can occur, with either $\Delta\Psi = 0°$ or $\Delta\Psi = 360°$ after half a rotation of the polarizer $P(\phi_1)$. This implies that on moving the state A across the Poincaré sphere a continuous change from one type of behavior to another is not possible. A discontinuous change in behavior can only occur when the geometric phase Ψ is singular. This happens when the first state A and the second state B are directly opposite to each other on the Poincaré sphere (and form a pair of "anti-podal points"). They are then orthogonal and the phase of the final state E is singular.[21] Indeed, when the state A lies on the equator ($\theta_A = 0$) then $\Psi = 2\phi_2 - \phi_1$, or $\Psi = 2\phi_2 - \phi_1 + \pi$, except when A and B are opposite. In that case Ψ is singular and undergoes a π phase jump. In Fig. 12 this occurs for the point ($\alpha_A = \pi/4, \theta_A = 0$) at which all the different phase contours intersect. In other words, when A moves across the equator, the geometric phase as a function of the angle ϕ_1 is singular and a transition from one type of behavior (with $\Delta\Psi = 360°$) to another type (with $\Delta\Psi = 0°$) occurs. This singular behavior, resulting in a 180° discontinuity of the geometric phase was indeed observed, see Fig. 13. Notice that although the depicted jump equals 180°, in our experiment it cannot be discerned from a −180° discontinuity. Whereas a positive jump results in $\Delta\Psi = 360°$ after a 180° rotation of the first polarizer, a negative jump yields $\Delta\Psi = 0°$. In that sense the singular behavior forms an intermediate step between the two dependencies shown in Figs. 10 and 11.

The ability to produce a 180° phase jump by means of a much smaller variation in ϕ_1 can be employed to cause a change from constructive interference to deconstructive interference when the beam is combined with a reference beam. Clearly, such a scheme can be used for fast optical switching.[22]

7. CONCLUSIONS

In summary, we have shown how the Pancharatnam connection may be interpreted geometrically. Our work offers an geometry-based approach to calculate the Pancharatnam-Berry phase associated with non-cyclic polarization changes. As such it is an alternative to the algebraic treatments presented earlier.[9,10] Our approach can be extended to the description of geometric phases in quantum mechanical systems.

We have also presented a new Mach-Zehnder-type setup with which the geometric phase that accompanies non-cyclic polarization changes can be observed. The geometric phase can exhibit linear, nonlinear or singular behavior. Excellent agreement between the predicted and observed behavior was obtained.

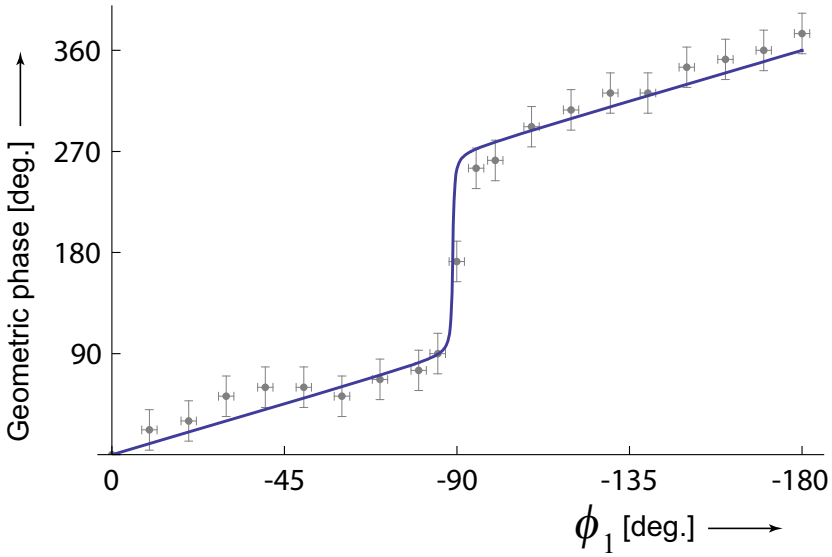

Figure 13. Singular behavior of the geometric phase of the final state E when the initial state A lies on the equator, as a function of the orientation angle ϕ_1. The solid curve is a theoretical prediction [Eq. (28)], the dots and error bars represent measurements. In this example $\theta_A = 0.27$, $\alpha_A = 0.0$ and $\phi_2 = 0$.

Acknowledgements

The authors wish to thank Laura de Graaff and Jacques Bouma for technical assistance, and The Netherlands Foundation for Fundamental Research of Matter (FOM) for financial support. TvD is supported by the Netherlands Organisation for Scientific Research (NWO) through a "Toptalent scholarship.

REFERENCES

[1] M.V. Berry, Proc. R. Soc. Lond. **A 392**, 45 (1984).
[2] M.V. Berry, Physics Today **43** (no. 12), 34 (1990).
[3] S. Pancharatnam, Proc. Indian Acad. Sci. A **44**, 247 (1956).
[4] M. Born and E. Wolf, *Principles of Optics* , 7^{th} ed. (Cambridge University Press, Cambridge, 1999).
[5] M.V. Berry, J. Mod. Optics **34**, 1401 (1987).
[6] R. Bhandari, Phys. Rep. **281**, 1 (1997).
[7] P. Hariharan, in: *Progress in Optics* (E. Wolf, ed.), vol. **48**, 149 (Elsevier, Amsterdam, 2005).
[8] R. Bhandari and J. Samuel, Phys. Rev. Lett. **60**, 1211 (1988).
[9] J. Samuel and R. Bhandari, Phys. Rev. Lett. **60**, 2339 (1988).
[10] T.F. Jordan, Phys. Rev. A **38**, 1590 (1988).
[11] R.C. Jones, J. Opt. Soc. Am. **31**, 488 (1941).
[12] F. Eriksson, Math. Mag. **63**, 184 (1990).
[13] L.E.J. Brouwer, Math. Ann. **LXXI**, 97 (1912).
[14] T.H. Chyba, L.J. Wang, L. Mandel and R. Simon, Opt. Lett. **13**, 562 (1988).
[15] H. Schmitzer, S. Klein and W. Dultz, Phys. Rev. Lett. **71**, 1530 (1993).
[16] R. Bhandari, Phys. Lett. A **171**, 262 (1992).
[17] R. Bhandari, Phys. Lett. A **171**, 267 (1992).
[18] T. van Dijk, H.F. Schouten, W. Ubachs and T.D. Visser, submitted.
[19] C. Brosseau, *Fundamentals of Polarized Light* (Wiley, New York, 1998).
[20] A.G. Wagh and V.C. Rakhecha, Phys. Lett. A **197**, 107 (1995).
[21] J.F. Nye, *Natural Focusing and Fine Structure of Light* (IOP Publishing, Bristol, 1999).
[22] G.I. Papadimitriou, C. Papazoglou and A.S. Pomportsis, *Optical Switching* (Wiley, Hoboken, 2007).